

Virtual Mixup Training for Unsupervised Domain Adaptation

Xudong Mao^{1*} Yun Ma^{1*} Zhenguo Yang¹ Yangbin Chen² Qing Li¹

¹Department of Computing, The Hong Kong Polytechnic University

²Department of Computer Science, City University of Hong Kong

xudong.xdmao@gmail.com mayun371@gmail.com

yzgcityu@gmail.com robinchen2-c@my.cityu.edu.hk

csqli@comp.polyu.edu.hk

Abstract

We study the problem of unsupervised domain adaptation which aims to adapt models trained on a labeled source domain to a completely unlabeled target domain. Recently, the cluster assumption has been applied to unsupervised domain adaptation and achieved strong performance. One critical factor in successful training of the cluster assumption is to impose the locally-Lipschitz constraint to the model. Existing methods only impose the locally-Lipschitz constraint around the training points while miss the other areas, such as the points in-between training data. In this paper, we address this issue by encouraging the model to behave linearly in-between training points. We propose a new regularization method called Virtual Mixup Training (VMT), which is able to incorporate the locally-Lipschitz constraint to the areas in-between training data. Unlike the traditional mixup model, our method constructs the combination samples without using the label information, allowing it to apply to unsupervised domain adaptation. The proposed method is generic and can be combined with most existing models such as the recent state-of-the-art model called VADA. Extensive experiments demonstrate that VMT significantly improves the performance of VADA on six domain adaptation benchmark datasets. For the challenging task of adapting MNIST to SVHN, VMT can improve the accuracy of VADA by over 30%. Code is available at <https://github.com/xudonmao/VMT>.

Introduction

Deep neural networks have launched a profound reformation in a wide variety of fields such as image classification (Krizhevsky, Sutskever, and Hinton 2012), detection (Girshick et al. 2014), and segmentation (Long, Shelhamer, and Darrell 2015). However, the performance of deep neural networks is often based on large amounts of labeled training data. In real-world tasks, generating labeled training data can be very expensive and may not always be feasible. One approach to this problem is to learn from a related labeled source data and generalize to the unlabeled target data, which is known as domain adaptation. In this work, we consider the problem of unsupervised domain adaptation where the training samples in the target domain are completely unlabeled.

*indicates equal contribution

For unsupervised domain adaptation, Ganin et al. (2016) proposed the domain adversarial training to learn domain-invariant features between the source and target domains, which has been a basis for numerous domain adaptation methods (Tzeng et al. 2017; Kumar et al. 2018; Shu et al. 2018; Saito et al. 2018; Xie et al. 2018). Most of the follow-up studies focus on how to learn better-aligned domain-invariant features, including the approaches of adversarial discriminative adaptation (Tzeng et al. 2017), maximizing classifier discrepancy (Saito et al. 2018), and class conditional alignment (Xie et al. 2018; Kumar et al. 2018).

Recently, Shu et al. (2018) have successfully incorporated the cluster assumption (Grandvalet and Bengio 2005) into the framework of domain adversarial training by adopting the conditional entropy loss. They also pointed out that the locally-Lipschitz constraint is critical to the performance of the cluster assumption. Without the locally-Lipschitz constraint, the classifier may abruptly change its predictions in the vicinity of the training samples. This will push the decision boundary close to the high-density regions, which violates the cluster assumption. To this end, they adopted virtual adversarial training (Miyato et al. 2018) to constrain the local Lipschitzness of the classifier.

However, virtual adversarial training only incorporates the locally-Lipschitz constraint to the training points while misses the other areas. To this end, we propose a new regularization method called Virtual Mixup Training (VMT), which is able to regularize the areas in-between training points to be locally-Lipschitz. In general, VMT extends mixup (Zhang et al. 2018) by replacing the real labels with virtual labels (i.e., the predicted labels by the classifier), allowing it to apply to unsupervised domain adaptation. Our proposed method is based on the fact that mixup favors linear behavior in-between training samples (Zhang et al. 2018). The idea of VMT is simple yet powerful: as Figure 1(a) shows, for the center point, different pairs of training samples make it behave linearly in different directions, and we can easily verify that if the model is linear in all directions at the center point, then the model is locally-Lipschitz at this center point. On the other hand, the locally-Lipschitz constraint is beneficial for pushing the decision boundary away from the high-density regions,

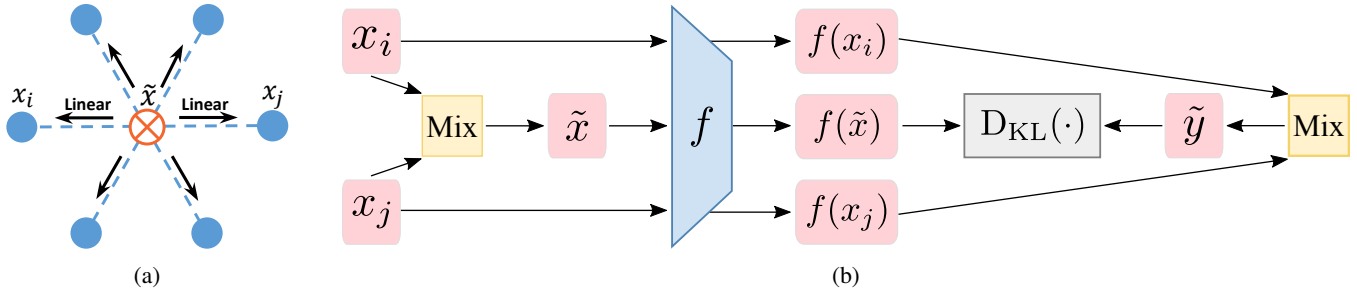


Figure 1: (a) Illustration of VMT, where blue points denote the training samples and the center point is in the area in-between training samples. For the center point, different pairs of training samples make it behave linearly in different directions, thus regularizing the center point to be locally-Lipschitz. (b) The framework of VMT, where f is a classifier and $D_{\text{KL}}(\cdot)$ denotes the KL-divergence.

which favors the cluster assumption (Ben-David et al. 2010; Shu et al. 2018).

Specifically, as shown in Figure 1(b), we first construct convex combinations, denoted as (\tilde{x}, \tilde{y}) , of pairs of training samples and their virtual labels, and then define a penalty term that punishes the difference between the combined sample’s prediction $f(\tilde{x})$ and the combined virtual label \tilde{y} . This penalty term encourages a linear change of the output distribution in-between training samples.

In practice, Shu et al. (2018) pointed out that the conditional entropy loss sometimes behaves unstably and even finds a degenerate solution for some challenging tasks, which also occurs in our model. To tackle this problem, we propose to mixup on the logits (i.e., the input of the softmax layer) instead of the probabilities (i.e., the output of the softmax layer). We argue that the problem of mixup on probabilities is that most of the probability values will tend to be zero since the targets are one-hot vectors, while the logits still have non-zero values.

In the experiments, we combine VMT with a recent state-of-the-art model called VADA (Shu et al. 2018), and evaluate on six commonly used benchmark datasets. The experimental results show that VMT is able to improve the performance of VADA for all tasks. For the most challenging task, MNIST \rightarrow SVHN without instance normalization, our model improves over VADA by 33.6%.

Our contributions can be summarized as follows:

- We propose the Virtual Mixup Training (VMT), a new regularization method, to impose the locally-Lipschitz constraint to the areas in-between training data.
- We propose to mixup on logits rather than mixup on probabilities to further improve the performance and training stability of VMT.
- We evaluate VMT on six benchmark datasets, and the experimental results demonstrate that VMT can achieve state-of-the-art performance on all the six datasets.

Related Work

Domain Adaptation Domain adaptation has gained extensive attention in recent years due to its advantage of utilizing unlabeled data. A theoretical analysis of domain adap-

tation was presented in (Ben-David et al. 2010). Early works (Shimodaira 2000) tried to minimize the discrepancy distance between the source and target feature distributions. Long et al. (2015) and Sun & Saenko (2016) extended this method by matching higher-order statistics of the two distributions. Huang et al. (2007), Tzeng et al. (2015), and Ganin et al. (2016) proposed to project the source and target feature distributions into some common space and match the learned features as close as possible. Specifically, Ganin et al. (2016) proposed the domain adversarial training to learn domain-invariant features, which has been a basis of numerous domain adaptation methods (Tzeng et al. 2017; Saito et al. 2018; Xie et al. 2018; Shu et al. 2018; Kumar et al. 2018). Tzeng et al. (2017) generalized a framework based on domain adversarial training and proposed to combine the discriminative model and GAN loss (Goodfellow et al. 2014). Saito et al. (2018) proposed to utilize two different classifiers to learn not only domain-invariant but also class-specific features. Shu et al. (2018) proposed to combine the cluster assumption (Grandvalet and Bengio 2005) with domain adversarial training. They also adopted virtual adversarial training (Miyato et al. 2018) to constrain the local Lipschitzness of the classifier, as they found that the locally-Lipschitz constraint is critical to the performance of the cluster assumption. Kumar et al. (2018) extended (Shu et al. 2018) to align class-specific features by using co-regularization (Sindhwani, Niyogi, and Belkin 2005). We also follow the line of (Shu et al. 2018) and propose a new method to impose the locally-Lipschitz constraint to the areas in-between training data. There are also many other promising models including domain separation networks (Bousmalis et al. 2016a), reconstruction-classification networks (Ghifary et al. 2016), tri-training (Saito, Ushiku, and Harada 2017), self-ensembling (French, Mackiewicz, and Fisher 2018), and image-to-image translation (Bousmalis et al. 2017).

Local Lipschitzness Grandvalet and Bengio (2005) pointed out that the local Lipschitzness is critical to the performance of the cluster assumption. Ben-David and Uner (2014) also showed in theory that Lipschitzness can be viewed as a way of formalizing the cluster assumption. Constraining local Lipschitzness has been proven as effective

in semi-supervised learning (Sajjadi, Javanmardi, and Tasdizen 2016; Laine and Aila 2017; Miyato et al. 2018) and domain adaptation (French, Mackiewicz, and Fisher 2018; Shu et al. 2018). In general, these methods smooth the output distribution of the model by constructing surrounding points of the training points and enforcing consistent predictions between the surrounding and training points. Specifically, Sajjadi, Javanmardi, and Tasdizen (2016), and Laine & Aila (2017) utilized the randomness of neural networks to construct the surrounding points. French, Mackiewicz, and Fisher (2018) proposed to construct two different networks and enforce the two networks to output consistent predictions for the same input. Miyato et al. (2018) utilized the adversarial examples (Goodfellow, Shlens, and Szegedy 2015) to regularize the model from the direction violating the local Lipschitzness mostly.

Mixup Zhang et al. (2018) proposed a regularization method called mixup to improve the generalization of neural networks. Mixup generates convex combinations of pairs of training examples and their labels, favoring the smoothness of the output distribution. A similar idea was presented in (Tokozume, Ushiku, and Harada 2018) for image classification. Verma et al. (2018) extended mixup by mixing on the output of a random hidden layer. Guo, Mao, and Zhang (2019) proposed to learn the mixing policy by an additional network instead of the random policy. A similar idea to ours was described in (Verma et al. 2019) for semi-supervised learning. They also used mixup to provide consistent predictions between unlabeled training samples. Berthelot et al. (2019) extended this method by mixing between the labeled and unlabeled samples.

Virtual Labels Virtual (or pseudo) labels have been widely used in semi-supervised learning (Miyato et al. 2018) and domain adaptation (Chen, Weinberger, and Blitzer 2011; Saito, Ushiku, and Harada 2017; Xie et al. 2018). In particular, Chen, Weinberger, and Blitzer (2011) and Saito, Ushiku, and Harada (2017) proposed to first use multiple classifiers to assign virtual labels to the target samples, and then train the classifier using the target samples with virtual labels. Xie et al. (2018) proposed to calculate the class centroids of the virtual labels to reduce the bias caused by the false virtual labels. The most related method to ours is virtual adversarial training (Miyato et al. 2018). Virtual adversarial training enforces the virtual labels of the original sample and its adversarial example to be similar, which can be used to impose the locally-Lipschitz constraint to the training samples.

Preliminaries

Domain Adversarial Training

We first describe domain adversarial training (Ganin et al. 2016) which is a basis of our model. Let \mathcal{X}_s and \mathcal{Y}_s be the distributions of the input sample x and label y from the source domain, and let \mathcal{X}_t be the input distribution of the target domain. Suppose a classifier $f = h \circ g$ can be decomposed into a feature encoder g and an embedding classifier h . The input x is first mapped through the feature encoder $g : \mathcal{X} \rightarrow \mathcal{Z}$, and then through the embedding classifier

$h : \mathcal{Z} \rightarrow \mathcal{Y}$. On the other hand, a domain discriminator $d : \mathcal{Z} \rightarrow (0, 1)$ maps the feature vector to the domain label $(0, 1)$. The domain discriminator d and feature encoder g are trained adversarially: d tries to distinguish whether the input sample x is from the source or target domain, while g aims to generate indistinguishable feature vectors of samples from the source and target domains. The objective of domain adversarial training can be formalized as follows:

$$\begin{aligned} \min_f \mathcal{L}_y(f; \mathcal{X}_s, \mathcal{Y}_s) + \lambda_d \mathcal{L}_d(g; \mathcal{X}_s, \mathcal{X}_t), \\ \mathcal{L}_y(f; \mathcal{X}_s, \mathcal{Y}_s) = -\mathbb{E}_{(x,y) \sim (\mathcal{X}_s, \mathcal{Y}_s)} [y^\top \ln f(x)], \\ \mathcal{L}_d(g; \mathcal{X}_s, \mathcal{X}_t) = \sup_d \mathbb{E}_{x \sim \mathcal{X}_s} [\ln d(g(x))] + \\ \mathbb{E}_{x \sim \mathcal{X}_t} [\ln(1 - d(g(x)))] , \end{aligned} \quad (1)$$

where λ_d is used to adjust the weight of \mathcal{L}_d .

Cluster Assumption

The cluster assumption states that the input data contains clusters, and if samples are in the same cluster, they come from the same class (Grandvalet and Bengio 2005). It has been widely used in semi-supervised learning (Grandvalet and Bengio 2005; Sajjadi, Javanmardi, and Tasdizen 2016; Miyato et al. 2018), and recently has been applied to unsupervised domain adaptation (Shu et al. 2018). The conditional entropy minimization is usually adopted to enforce the behavior of the cluster assumption (Grandvalet and Bengio 2005; Sajjadi, Javanmardi, and Tasdizen 2016; Miyato et al. 2018; Shu et al. 2018):

$$\mathcal{L}_c(f; \mathcal{X}_t) = -\mathbb{E}_{x \sim \mathcal{X}_t} [f(x)^\top \ln f(x)]. \quad (2)$$

Local Lipschitzness

We first recall the definition of local Lipschitzness:

Definition 1. (Local Lipschitzness) We say a function $f : \mathcal{X} \rightarrow \mathcal{Y}$ is locally-Lipschitz, if for each $x_0 \in \mathcal{X}$, there exists constants $L > 0$ and $\delta_0 > 0$ such that $\|f(x) - f(x_0)\| \leq L\|x - x_0\|$ holds for all $\|x - x_0\| < \delta_0$, $x \in \mathcal{X}$.

Shu et al. (2018) pointed out that the locally-Lipschitz constraint is critical to the performance of the cluster assumption, and adopted virtual adversarial training (Miyato et al. 2018) to impose the locally-Lipschitz constraint:

$$\mathcal{L}_v(f; \mathcal{X}) = \mathbb{E}_{x \sim \mathcal{X}} \left[\max_{\|r\| \leq \epsilon} \text{D}_{\text{KL}}(f(x) \| f(x+r)) \right]. \quad (3)$$

Virtual Mixup Training

Shu et al. (2018) adopted two methods, including the conditional entropy (Eq. 2) and virtual adversarial training (Eq. 3), to enforce the cluster assumption. Minimizing the conditional entropy forces the classifier to be confident on the training points, thus driving the decision boundary away from the high-density regions. On the other hand, virtual adversarial training imposes the locally-Lipschitz constraint to the training points, and the locally-Lipschitz constraint can favor the cluster assumption, because it prevents the classifier to abruptly change its predictions in the vicinity of the training points, thus driving the decision boundary away

from the high-density regions. However, both the conditional entropy and virtual adversarial training only consider the areas around the training points while miss the other areas such as the points in-between training data. To remedy this problem, we propose the Virtual Mixup Training (VMT), which is able to incorporate the locally-Lipschitz constraint to the areas in-between training data.

The original mixup (Zhang et al. 2018) model has shown the ability to enforce the classifier to behave linearly in-between training samples by applying the following convex combinations of labeled samples:

$$\begin{aligned}\tilde{x} &= \lambda x_i + (1 - \lambda)x_j, \\ \tilde{y} &= \lambda y_i + (1 - \lambda)y_j.\end{aligned}\quad (4)$$

However, for unsupervised domain adaptation, we have no direct information about y_i and y_j of the target domain. Inspired by (Miyato et al. 2018), we replace y_i and y_j with the approximations, $f(x_i)$ and $f(x_j)$, which are the current predictions by the classifier f . Literally, we call $f(x_i)$ and $f(x_j)$ virtual labels, and formalize our proposed VMT as follows:

$$\begin{aligned}\tilde{x} &= \lambda x_i + (1 - \lambda)x_j, \\ \tilde{y} &= \lambda f(x_i) + (1 - \lambda)f(x_j),\end{aligned}\quad (5)$$

where $\lambda \sim \text{Beta}(\alpha, \alpha)$, for $\alpha \in (0, \infty)$. Then we penalize the difference between the prediction $f(\tilde{x})$ and the virtual label \tilde{y} :

$$\mathcal{L}_m(f; \mathcal{X}) = \mathbb{E}_{x \sim \mathcal{X}} [\text{D}_{\text{KL}}(\tilde{y} \| f(\tilde{x}))]. \quad (6)$$

Like the original mixup, our proposed VMT also encourages the classifier f to behave linearly between x_i and x_j . Moreover, as shown in Figure 1(a), for the virtual point \tilde{x} , different pairs of x_i and x_j enforce it to behave linearly in different directions, and we can verify that if f is linear in all directions at \tilde{x} , then f is locally-Lipschitz at \tilde{x} . We prove the linear behavior and the local Lipschitzness of VMT in the Appendix. We also empirically verify this by plotting in Figure 2 the gradient norms of VADA and VMT in-between training samples, since the gradient norm is an indicator of the local Lipschitzness (Hein and Andriushchenko 2017). It shows that VMT has much smaller gradient norms than VADA.

The proposed VMT is generic and can be combined with most existing models. In particular, we can combine VMT with a recent state-of-the-art model, VADA, which then leads us to the following objective:

$$\begin{aligned}\min_f \mathcal{L}_{y,d} + \lambda_s [\mathcal{L}_m(f; \mathcal{X}_s) + \mathcal{L}_v(f; \mathcal{X}_s)] + \\ \lambda_t [\mathcal{L}_m(f; \mathcal{X}_t) + \mathcal{L}_v(f; \mathcal{X}_t) + \mathcal{L}_c(f; \mathcal{X}_t)],\end{aligned}\quad (7)$$

where $\mathcal{L}_{y,d} = \mathcal{L}_y(f; \mathcal{X}_s, \mathcal{Y}_s) + \lambda_d \mathcal{L}_d(g; \mathcal{X}_s, \mathcal{X}_t)$ and (λ_s, λ_t) are used to adjust the weights of the penalty terms on the source and target domains. Note that we also incorporate virtual adversarial training in Eq. 7, and empirically show in the experiments that VMT is orthogonal to virtual adversarial training for most tasks. For the source domain, we also replace y_i and y_j with the virtual labels, without using the label information.

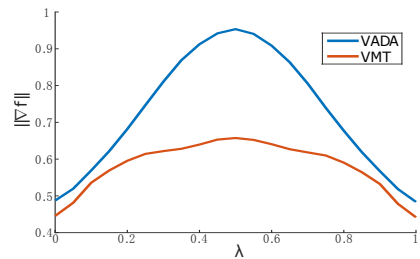


Figure 2: Gradient norms of the classifier f with respect to the input in-between training samples: $\tilde{x} = \lambda x_i + (1 - \lambda)x_j$. Both models are trained with the same architecture and evaluated on the whole test set. VMT has much smaller gradient norms than VADA.

Like the original mixup, the implementation of VMT is also simple and straightforward. One important advantage of VMT is the low computational cost, and we show in the experiments that VMT has a much lower computational cost than virtual adversarial training. Despite its simplicity, VMT achieves a new state-of-the-art performance on several benchmark datasets.

Mixup on Logits

As stated in (Shu et al. 2018), VADA shows high-variance results for some tasks and even finds a degenerate solution quickly. In practice, we also observe that Eq. 5 sometimes collapse to a degenerate solution. To tackle this problem, we propose to mixup-on-logits (i.e., the input of the softmax layer) instead of mixup-on-probabilities (i.e., the output of the softmax layer), which is also studied in literature (Daniel Varga 2017) for supervised learning. Let f_{logits} denote the layers before the softmax layer and f_{softmax} denote the softmax layer. Then Eq. 5 is modified as:

$$\tilde{y} = f_{\text{softmax}}(\lambda f_{\text{logits}}(x_i) + (1 - \lambda)f_{\text{logits}}(x_j)). \quad (8)$$

The problem of mixup-on-probabilities is that most of the probabilities will tend to be zero since the targets are one-hot vectors, and mixup between zeros vanishes the effect of favoring linear behavior. This problem does not arise in mixup-on-logits because the logits still have non-zero values even though the probabilities are close to zero. In the experiments, we empirically verify that mixup-on-logits performs more stably than mixup-on-probabilities, especially for the challenging task of MNIST \rightarrow SVHN.

Experiments

In our experiments, we focus on the visual domain adaptation and evaluate our model on six benchmark datasets including MNIST, MNIST-M, Synthetic Digits (SYN), Street View House Numbers (SVHN), CIFAR-10, and STL-10.

Iterative Refinement Training

Following VADA, we also perform an iterative refinement training technique called DIRT-T (Shu et al. 2018) for further optimizing the cluster assumption on the target domain. Specifically, we first initialize with a trained VMT model

Source Target	MNIST SVHN	SVHN MNIST	MNIST MNIST-M	SYN SVHN	CIFAR STL	STL CIFAR
MMD (Long et al. 2015)	-	71.1	76.9	88.0	-	-
DANN (Ganin et al. 2016)	35.7	71.1	81.5	90.3	-	-
DRCN (Ghifary et al. 2016)	40.1	82.0	-	-	66.4	58.7
DSN (Bousmalis et al. 2016b)	-	82.7	83.2	91.2	-	-
kNN-Ad (Sener et al. 2016)	40.3	78.8	86.7	-	-	-
PixelDA (Bousmalis et al. 2017)	-	-	98.2	-	-	-
ATT (Saito, Ushiku, and Harada 2017)	52.8	86.2	94.2	92.9	-	-
PI-model (aug) (French, Mackiewicz, and Fisher 2018)	71.4	92.0	-	94.2	76.3	64.2
Without Instance-Normalized Input:						
Source-Only	27.9	77.0	58.5	86.9	76.3	63.6
VADA (Shu et al. 2018)	47.5	97.9	97.7	94.8	80.0	73.5
Co-DA (Kumar et al. 2018)	55.3	98.8	99.0	96.1	81.4	76.4
VMT (ours)	59.3	98.8	99.0	96.2	82.0	80.2
VADA + DIRT-T (Shu et al. 2018)	54.5	99.4	98.9	96.1	-	75.3
Co-DA + DIRT-T (Kumar et al. 2018)	63.0	99.4	99.1	96.5	-	77.6
VMT + DIRT-T (ours)	88.1	99.5	99.1	96.5	-	80.6
With Instance-Normalized Input:						
Source-Only	40.9	82.4	59.9	88.6	77.0	62.6
VADA (Shu et al. 2018)	73.3	94.5	95.7	94.9	78.3	71.4
Co-DA (Kumar et al. 2018)	81.7	98.7	98.0	96.0	80.6	74.7
VMT (ours)	85.2	98.9	98.0	96.4	81.3	79.5
VADA + DIRT-T (Shu et al. 2018)	76.5	99.4	98.7	96.2	-	73.3
Co-DA + DIRT-T (Kumar et al. 2018)	88.0	99.4	98.8	96.5	-	75.9
VMT + DIRT-T (ours)	95.1	99.4	98.9	96.6	-	80.2

Table 1: Test set accuracy on the visual domain adaptation benchmark datasets. For all tasks, VMT improves the accuracy of VADA and achieves the state-of-the-art performance.

using Eq. 7, and then iteratively minimize the following objective on the target domain:

$$\min_{f_n} \lambda_t \mathcal{L}_t(f_n; \mathcal{X}_t) + \beta \mathbb{E}[\mathbf{D}_{\text{KL}}(f_{n-1}(x) \| f_n(x))], \quad (9)$$

where $\mathcal{L}_t = \mathcal{L}_m + \mathcal{L}_v + \mathcal{L}_c$. In practice, for the initialization model, we do not need to train the VMT model until convergence, and pre-training for 40000 or 80000 iterations is enough to achieve good performance. We report the results of using and without using DIRT-T in the following experiments.

Hyperparameters

Following (Shu et al. 2018), we tune the four hyperparameters $(\lambda_d, \lambda_s, \lambda_t, \beta)$ by randomly selecting 1000 labeled target samples from the training set as the validation set. We restrict the hyperparameter search to $\lambda_d = \{0, 0.01\}$, $\lambda_s = \{0, 1\}$, $\lambda_t = \{0.01, 0.02, 0.04, 0.06, 0.08, 0.1, 1\}$, and $\beta = \{0.001, 0.01, 0.1, 1\}$; α in Eq. 5 is fixed as 1 for all experiments. A complete list of the hyperparameters is presented in the Appendix.

Compared with VADA, the main different setting is λ_t . We empirically find that increasing the value of λ_t is able to improve the performance significantly. But for VADA, it will

collapse to a degenerate solution if we set the same value of λ_t .

Implementation Detail

Architecture We use the same network architectures as the ones in VADA(Shu et al. 2018) for a fair comparison. In particular, a small CNN is used for the tasks of digits, and a larger CNN is used for the tasks between CIFAR-10 and STL-10.

Baselines We primarily compare our model with two baselines: VADA (Shu et al. 2018) and Co-DA (Kumar et al. 2018). Also based on VADA, Co-DA used a co-regularization method to make a better domain alignment. We also show the results of several other recently proposed unsupervised domain adaptation models for comparison.

Others Following (Shu et al. 2018), we replace gradient reversal (Ganin et al. 2016) with the adversarial training (Goodfellow et al. 2014) of alternating updates between the domain discriminator and feature encoder. We also follow (Shu et al. 2018) to apply the instance normalization to the input images, and report the results of using or without using the instance normalization. The implementation of our

MNIST \rightarrow SVHN without Instance-Normalized Input:											Average
VMT@40K	57.7	57.6	57.4	50.1	54.1	50.0	52.7	40.1	53.9	45.5	51.9 ± 5.7
VMT@160K	64.6	64.6	58.3	61.4	57.3	63.7	64.5	49.4	56.9	52.0	59.3 ± 5.5
VMT + DIRT-T@160K	95.9	95.9	95.3	95.3	95.1	83.6	82.8	80.4	79.9	76.6	88.1 ± 8.0
MNIST \rightarrow SVHN with Instance-Normalized Input:											Average
VMT@40K	86.1	85.6	86.1	85.8	85.2	85.6	84.3	84.0	84.5	84.3	85.2 ± 0.8
VMT + DIRT-T@160K	96.0	95.9	95.6	95.5	95.4	95.3	95.3	95.1	94.2	92.8	95.1 ± 1.0

Table 2: Test set accuracies of 10 runs at difference stages of training. VMT@40K denotes the accuracy of VMT at iteration 40000. DIRT-T takes the VMT@40K model as the initialization model. Our model shows small variance in performance for the task with instance normalization, while shows moderate variance for the task without instance normalization.

MNIST \rightarrow SVHN without Instance-Normalized Input:											Average
VMT _{prob} @40K	47.5	54.0	50.1	49.6	50.5	50.2	44.8	48.1	38.4	43.1	47.6 ± 4.5
VMT _{prob} @160K	59.2	62.3	61.0	60.0	60.3	65.3	57.0	60.4	21.7	51.1	55.8 ± 12.5
VMT _{prob} + DIRT-T@160K	95.0	94.4	93.3	91.9	89.7	88.5	78.3	77.6	19.6	15.6	74.4 ± 30.6

Table 3: Test set accuracies of VMT with mixup-on-probabilities. The results indicate high variance in performance. The model sometimes behaves unstably and collapses to a degenerate solution.

model is based on the official implementation of VADA.

MNIST \rightarrow SVHN

We first evaluate VMT on the adaptation task from MNIST to SVHN, which is usually regarded as a challenging task (Ganin et al. 2016; Shu et al. 2018). It is especially difficult when the input is not instance-normalized.

Without Instance Normalization When not applying instance normalization, VADA removes the conditional entropy minimization during training, as it behaves unstably and finds a degenerate solution quickly (Shu et al. 2018). We find that this problem no longer exists in our model, and thus we keep the conditional entropy minimization during training. As Table 1 shows, when not applying DIRT-T, VMT outperforms VADA and Co-DA by 11.8% and 4%, respectively. When applying DIRT-T, VMT outperforms VADA and Co-DA by 33.6% and 25.1%, respectively.

The reported accuracies are averaged over 10 trials, and we list the complete results in Table 2. We have the following three observations from Table 2. First, the results indicate moderate variance in performance, but even in the worst-case (76.6%), it still outperforms VADA and Co-DA by 22.1% and 13.6%. Second, the best model can achieve an accuracy of 95.9%, which is very close to the one applying instance normalization to the input. Third, generally speaking, if the model shows good performance at iteration 40000, it usually can achieve good results for both the VMT model and DIRT-T model.

Note that the reported results of VMT and DIRT-T are both achieved at iteration 160000. Interestingly, if we continue to train the DIRT-T model, we observe an accuracy of 96.4% at iteration 260000. Moreover, we train a classifier

on the target domain (i.e., SVHN) with labels revealed using the same network architecture and same settings, and it is usually treated as an upper bound for domain adaptation models. This train-on-target model achieves an accuracy of 96.5%. Our model achieves a very close accuracy (96.4%) to the upper bound (96.5%).

The reported results are achieved under $\lambda_t = 0.01$. If we set λ_t to 0.02, VMT@160K generally performs better and can achieve an accuracy of 73.7% but sometimes collapses to a degenerate solution. More discussion about the performance of $\lambda_t = 0.02$ is provided in the Appendix.

With Instance Normalization When applying instance normalization, VMT + DIRT-T outperforms VADA and Co-DA by 18.6% and 7.1%, respectively. Moreover, we also show the results of 10 runs in Table 2. Different from the case without instance normalization, the results of applying instance normalization show small variance in performance. Note that compared with VADA, we set a larger $\lambda_t = 0.06$, which is able to improve the performance, while VADA will collapse to a degenerate solution if we set the same value of λ_t . We show the comparison results of VMT between $\lambda_t = 0.01$ and $\lambda_t = 0.06$ in the Appendix. Similar to the case without instance normalization, if we continue to train the DIRT-T model, VMT + DIRT-T can achieve an accuracy of 96.4% at iteration 280000.

Other Digits Adaptation Tasks

For the other digits adaptation tasks including SVHN \rightarrow MNIST, MNIST \rightarrow MNIST-M, and SYN DIGITS \rightarrow SVHN, the baselines already achieve high accuracies. As Table 1 shows, for these tasks, VMT still outperforms VADA and shows similar performance to Co-DA.

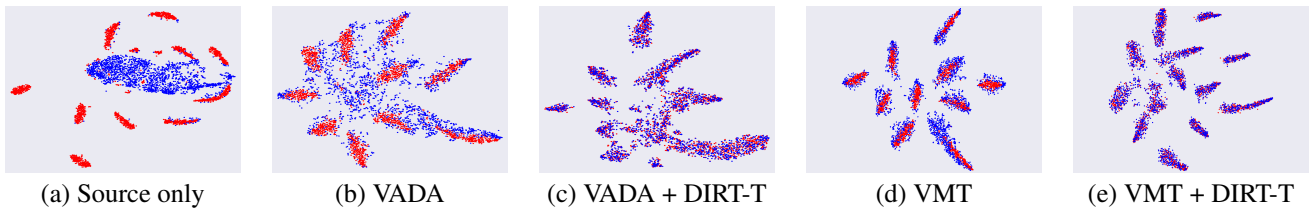


Figure 3: T-SNE visualization of the last hidden layer for MNIST (red) to SVHN (blue) without instance normalization. Compared with VADA, VMT generates closer features vectors for the source and target domains, and shows stronger clustering performance for the target domain. VMT + DIRT-T makes the source and target features closest.

CIFAR-10 \leftrightarrow STL-10.

For CIFAR-10 and STL-10, there are nine overlapping classes between the two datasets. Following (French, Mackiewicz, and Fisher 2018; Shu et al. 2018; Kumar et al. 2018), we remove the non-overlapping classes and remain the nine overlapping classes. STL-10 \rightarrow CIFAR-10 is more difficult than CIFAR-10 \rightarrow STL-10, as STL-10 has less labeled samples than CIFAR-10. We observe more significant gains for the harder task of STL-10 \rightarrow CIFAR-10. VMT outperforms VADA by 8.1% and 6.7%, and outperforms Co-DA by 4.8% and 3.8%, for with and without instance normalization, respectively. For CIFAR-10 \rightarrow STL-10, VMT improves over VADA by 3% and 2% for with and without instance normalization, respectively. Note that DIRT-T has no effect on this task, because STL-10 contains a very small training set, making it difficult to estimate the conditional entropy.

Mixup on Logits or Probabilities?

The inputs and outputs of the softmax layer are called logits and probabilities, respectively. In this experiment, we compare the performance of two schemas: mixup-on-logits (Eq. 8) and mixup-on-probabilities (Eq. 5). The results of mixup-on-logits and mixup-on-probabilities are shown in Table 2 and Table 3, respectively. We can observe that mixup-on-logits performs better and more stable than mixup on probabilities. Mixup-on-probabilities sometimes collapses to a degenerate solution whose accuracy is only 15.6%. Moreover, we have also investigated the performance of mixup on some intermediate layers in the Appendix, and mixup-on-logits achieves the best performance.

Comparing with Virtual Adversarial Training

Virtual adversarial training (VAT) (Miyato et al. 2018) is another approach to impose the locally-Lipschitz constraint, as used in VADA. We conduct comparison experiments between VAT (Eq. 3) and our proposed VMT (Eq. 6), and the results are shown in Table 4. VMT achieves higher accuracies than VAT for all the tasks, which demonstrates that VMT surpasses VAT in favoring the cluster assumption. Furthermore, combining VMT and VAT is able to further improve the performance except for CIFAR-10 \rightarrow STL-10. This shows that VMT is orthogonal to VAT for most tasks, and they can be used together to constrain the local Lipschitzness. Compared with VAT, another advantage of VMT is the low computational cost. For the task of MNIST \rightarrow SVHN with instance normalization, VMT costs about 100

Source Target	MNIST SVHN	MNIST MNISTM	SVHN SVHN	CIFAR STL	STL CIFAR	
With Instance-Normalized Input:						
\mathcal{L}_c	66.8	83.1	93.8	93.4	79.1	68.6
$\mathcal{L}_c, \mathcal{L}_v$	73.3	94.5	95.7	94.9	78.3	71.4
$\mathcal{L}_c, \mathcal{L}_m$	82.6	98.5	97.3	95.6	82.0	78.3
$\mathcal{L}_c, \mathcal{L}_v, \mathcal{L}_m$	85.2	98.9	98.0	96.4	81.3	79.5

Table 4: Test set accuracy in comparison experiments between VAT and VMT. \mathcal{L}_c denotes the conditional entropy loss, \mathcal{L}_v denotes the VAT loss, and \mathcal{L}_m denotes the VMT loss. $\{\mathcal{L}_c, \mathcal{L}_m\}$ means that we only use $\mathcal{L}_{y,d}$, \mathcal{L}_c , and \mathcal{L}_m in Eq. 7, and set the weights of the other losses to 0. The results of $\{\mathcal{L}_c\}$ and $\{\mathcal{L}_c, \mathcal{L}_v\}$ are duplicated from (Shu et al. 2018).

seconds for 1000 iterations in our GPU server, while VAT needs about 140 seconds. The dynamic comparison of the accuracy over time is presented in the Appendix.

Visualization of Representation

We further present the T-SNE visualization results in Figure 3. We use the most challenging task (i.e., MNIST \rightarrow SVHN without instance normalization) to highlight the differences. As shown in Figure 3, source-only training shows a discriminative clustering result for the source domain but generates only one cluster for the target domain. We can observe that VMT makes the features from the source and target domains much closer than VADA, and shows stronger clustering performance of the target samples than VADA does. VMT + DIRT-T can further get closer feature vectors of the source and target domains.

Conclusion

In this paper, we proposed a novel method called Virtual Mixup Training (VMT), for unsupervised domain adaptation. VMT is designed to constrain the local Lipschitzness to favor the cluster assumption. The idea of VMT is to make linearly-change predictions along the lines between pairs of training samples. We empirically show that VMT significantly improves the performance of the recent state-of-the-art model called VADA. For a challenging task of adapting MNIST to SVHN, VMT can outperform VADA by over 33.6%.

References

- Ben-David, S., and Uner, R. 2014. Domain adaptation—can quantity compensate for quality? *Annals of Mathematics and Artificial Intelligence* 70(3):185–202.
- Ben-David, S.; Blitzer, J.; Crammer, K.; Kulesza, A.; Pereira, F.; and Vaughan, J. W. 2010. A theory of learning from different domains. *Machine Learning*.
- Berthelot, D.; Carlini, N.; Goodfellow, I.; Papernot, N.; Oliver, A.; and Raffel, C. 2019. Mixmatch: A holistic approach to semi-supervised learning. *arXiv:1905.02249*.
- Bousmalis, K.; Trigeorgis, G.; Silberman, N.; Krishnan, D.; and Erhan, D. 2016a. Domain separation networks. In *NeurIPS*, 343–351.
- Bousmalis, K.; Trigeorgis, G.; Silberman, N.; Krishnan, D.; and Erhan, D. 2016b. Domain separation networks. In *NeurIPS*, 343–351.
- Bousmalis, K.; Silberman, N.; Dohan, D.; Erhan, D.; and Krishnan, D. 2017. Unsupervised pixel-level domain adaptation with generative adversarial networks. In *CVPR*.
- Chen, M.; Weinberger, K. Q.; and Blitzer, J. C. 2011. Co-training for domain adaptation. In *NeurIPS*, 2456–2464.
- Daniel Varga, Adrian Csiszarik, Z. Z. 2017. Gradient regularization improves accuracy of discriminative models. *arXiv:1712.09936*.
- French, G.; Mackiewicz, M.; and Fisher, M. 2018. Self-ensembling for visual domain adaptation. In *ICLR*.
- Ganin, Y.; Ustinova, E.; Ajakan, H.; Germain, P.; Larochelle, H.; Laviolette, F.; Marchand, M.; and Lempitsky, V. 2016. Domain-adversarial training of neural networks. *JMLR* 17(1):2096–2030.
- Ghifary, M.; Kleijn, W. B.; Zhang, M.; Balduzzi, D.; and Li, W. 2016. Deep reconstruction-classification networks for unsupervised domain adaptation. In *ECCV*, 597–613.
- Girshick, R.; Donahue, J.; Darrell, T.; and Malik, J. 2014. Rich feature hierarchies for accurate object detection and semantic segmentation. In *CVPR*.
- Goodfellow, I.; Pouget-Abadie, J.; Mirza, M.; Xu, B.; Warde-Farley, D.; Ozair, S.; Courville, A.; and Bengio, Y. 2014. Generative adversarial nets. In *NeurIPS*, 2672–2680.
- Goodfellow, I.; Shlens, J.; and Szegedy, C. 2015. Explaining and harnessing adversarial examples. In *ICLR*.
- Grandvalet, Y., and Bengio, Y. 2005. Semi-supervised learning by entropy minimization. In *NeurIPS*, 529–536.
- Guo, H.; Mao, Y.; and Zhang, R. 2019. Mixup as locally linear out-of-manifold regularization. In *AAAI*.
- Hein, M., and Andriushchenko, M. 2017. Formal guarantees on the robustness of a classifier against adversarial manipulation. In *NeurIPS*, 2266–2276.
- Huang, J.; Gretton, A.; Borgwardt, K.; Schölkopf, B.; and Smola, A. J. 2007. Correcting sample selection bias by unlabeled data. In *NeurIPS*, 601–608.
- Krizhevsky, A.; Sutskever, I.; and Hinton, G. E. 2012. Imagenet classification with deep convolutional neural networks. In *NeurIPS*, 1097–1105.
- Kumar, A.; Sattigeri, P.; Wadhawan, K.; Karlinsky, L.; Feris, R.; Freeman, B.; and Wornell, G. 2018. Co-regularized alignment for unsupervised domain adaptation. In *NeurIPS*.
- Laine, S., and Aila, T. 2017. Temporal ensembling for semi-supervised learning. In *ICLR*.
- Long, M.; Cao, Y.; Wang, J.; and Jordan, M. I. 2015. Learning transferable features with deep adaptation networks. In *ICML*, 97–105.
- Long, J.; Shelhamer, E.; and Darrell, T. 2015. Fully convolutional networks for semantic segmentation. In *CVPR*.
- Miyato, T.; ichi Maeda, S.; Koyama, M.; and Ishii, S. 2018. Virtual adversarial training: A regularization method for supervised and semi-supervised learning. *TPAMI*.
- Saito, K.; Watanabe, K.; Ushiku, Y.; and Harada, T. 2018. Maximum classifier discrepancy for unsupervised domain adaptation. In *CVPR*.
- Saito, K.; Ushiku, Y.; and Harada, T. 2017. Asymmetric tri-training for unsupervised domain adaptation. In *ICML*.
- Sajjadi, M.; Javanmardi, M.; and Tasdizen, T. 2016. Regularization with stochastic transformations and perturbations for deep semi-supervised learning. In *NeurIPS*, 1163–1171.
- Sener, O.; Song, H. O.; Saxena, A.; and Savarese, S. 2016. Learning transferrable representations for unsupervised domain adaptation. In *NeurIPS*, 2110–2118.
- Shimodaira, H. 2000. Improving predictive inference under covariate shift by weighting the log-likelihood function. *Journal of Statistical Planning and Inference* 227 – 244.
- Shu, R.; Bui, H.; Narui, H.; and Ermon, S. 2018. A DIRT-t approach to unsupervised domain adaptation. In *ICLR*.
- Sindhwani, V.; Niyogi, P.; and Belkin, M. 2005. Unsupervised domain adaptation by backpropagation. In *Workshop on Learning with Multiple Views, ICML*.
- Sun, B., and Saenko, K. 2016. Deep coral: Correlation alignment for deep domain adaptation. In *ECCV Workshops*.
- Tokozume, Y.; Ushiku, Y.; and Harada, T. 2018. Between-class learning for image classification. In *CVPR*.
- Tzeng, E.; Hoffman, J.; Darrell, T.; and Saenko, K. 2015. Simultaneous deep transfer across domains and tasks. In *ICCV*.
- Tzeng, E.; Hoffman, J.; Saenko, K.; and Darrell, T. 2017. Adversarial discriminative domain adaptation. In *CVPR*.
- Verma, V.; Lamb, A.; Beckham, C.; Najafi, A.; Mitliagkas, I.; Courville, A.; Lopez-Paz, D.; and Bengio, Y. 2018. Manifold mixup: Better representations by interpolating hidden states. *arXiv:1806.05236*.
- Verma, V.; Lamb, A.; Kannala, J.; Bengio, Y.; and Lopez-Paz, D. 2019. Interpolation consistency training for semi-supervised learning. In *IJCAI*.
- Xie, S.; Zheng, Z.; Chen, L.; and Chen, C. 2018. Learning semantic representations for unsupervised domain adaptation. In *ICML*, 5423–5432.
- Zhang, H.; Cisse, M.; Dauphin, Y. N.; and Lopez-Paz, D. 2018. mixup: Beyond empirical risk minimization. In *ICLR*.

Appendix

Proof about the Linear Behavior of VMT

Lemma 1. Optimizing Eq. 6 encourages the classifier f to behave linearly between x_i and x_j .

Proof. Minimizing $\mathbb{E}_{x \sim \mathcal{X}} [\mathbf{D}_{\text{KL}}(\tilde{y} \| f(\tilde{x}))]$ enforces the classifier f to output \tilde{y} for \tilde{x} . If $\mathbb{E}_{x \sim \mathcal{X}} [\mathbf{D}_{\text{KL}}(\tilde{y} \| f(\tilde{x}))] = 0$, then (\tilde{x}, \tilde{y}) becomes a point on the classifier f .

$$\begin{aligned} \frac{\tilde{y} - y_1}{\tilde{x} - x_1} &= \frac{(1 - \lambda)(y_1 - y_2)}{(1 - \lambda)(x_1 - x_2)} = \frac{y_1 - y_2}{x_1 - x_2}, \\ \frac{\tilde{y} - y_2}{\tilde{x} - x_2} &= \frac{\lambda(y_1 - y_2)}{\lambda(x_1 - x_2)} = \frac{y_1 - y_2}{x_1 - x_2}. \end{aligned} \tag{10}$$

Eq. 10 indicates the same slope among x_1 , \tilde{x} , and x_2 . Therefore, optimizing $\mathbb{E}_{x \sim \mathcal{X}} [\mathbf{D}_{\text{KL}}(\tilde{y} \| f(\tilde{x}))]$ encourages the classifier f to behave linearly between x_i and x_j and we finish the proof. □

Proof about Imposing Locally-Lipschitz Constraint of VMT

Lemma 2. If f is linear in all directions at \tilde{x} , then f is locally-Lipschitz at \tilde{x} .

Proof. Since f is linear in all directions at \tilde{x} , we can assume a largest slope M for the surrounding points $\{x \in \mathcal{X} \mid \|x - \tilde{x}\| \leq \delta_0\}$ to \tilde{x} such that

$$\left\| \frac{f(x) - f(\tilde{x})}{x - \tilde{x}} \right\| \leq M. \tag{11}$$

Then we can get

$$\|f(x) - f(\tilde{x})\| \leq M\|x - \tilde{x}\|, \tag{12}$$

which implies the local Lipschitzness at \tilde{x} as in Definition 1, and we finish the proof. □

Hyperparameters

We restrict the hyperparameter search to $\lambda_d = \{0, 0.01\}$, $\lambda_s = \{0, 1\}$, $\lambda_t = \{0.01, 0.02, 0.04, 0.06, 0.08, 0.1, 1\}$, and $\beta = \{0.001, 0.01, 0.1, 1\}$. Compared with VADA, the main different setting is λ_t . We empirically find that increasing the value of λ_t is able to improve the performance significantly. But for VADA, it will collapse to a degenerate solution if we set the same value of λ_t . We set the refinement interval (Shu et al. 2018) of DIRT-T to 5000 iterations. The only exception is MNIST \rightarrow MNIST-M. For this special case, we set the refinement interval to 500, and set the weight of $\mathcal{L}_m(f; \mathcal{X}_t)$ to 10^{-3} . We use Adam Optimizer (learning rate = 0.001, $\beta_1 = 0.5$, $\beta_2 = 0.999$) with an exponential moving average (momentum = 0.998) to the parameter trajectory. When not applying DIRT-T, we train VMT for $\{40000, 80000, 160000\}$ iterations, with the number of iterations chosen as a hyperparameter. When applying DIRT-T, we train VMT for $\{40000, 80000\}$ iterations as the initialization model, and train DIRT-T for $\{40000, 80000, 160000\}$ iterations.

Task	Instance Normalization	λ_d	λ_s	λ_t	β
MNIST \rightarrow SVHN	Yes	0.01	1	0.06	0.01
MNIST \rightarrow SVHN	No	0.01	1	0.01	0.001
SVHN \rightarrow MNIST	Yes, No	0.01	0	0.1	0.01
MNIST \rightarrow MNIST-M	Yes, No	0.01	0	0.01	0.01
SYN \rightarrow SVHN	Yes, No	0.01	1	1	1
CIFAR \rightarrow STL	Yes, No	0	1	0.1	0.01
STL \rightarrow CIFAR	Yes, No	0	0	0.1	0.01

Table 5: List of the hyperparameters.

The Effect of λ_t for MNIST \rightarrow SVHN without Instance Normalization

In this experiment, we compare the performance between $\lambda_t = 0.02$ and $\lambda_t = 0.01$ for MNIST \rightarrow SVHN without Instance Normalization. We have the following four observations from Table 6. First, $\lambda_t = 0.02$ sometimes collapses to a degenerate solution whose accuracy is less than 20%. Second, when the model with $\lambda_t = 0.02$ collapses, the test set accuracy on the source domain is also very small. Thus we can exclude the collapsed model at the early stage of training by checking the test set accuracy on the source domain. Third, when not applying DIRT-T (VMT@160K in the table), $\lambda_t = 0.02$ outperforms $\lambda_t = 0.01$ significantly except for the case that $\lambda_t = 0.02$ collapses to a degenerate solution. Forth, when applying DIRT-T, $\lambda_t = 0.02$ and $\lambda_t = 0.01$ have similar performance.

MNIST \rightarrow SVHN without Instance-Normalized Input:											
VMT@40K:Source ($\lambda_t = 0.02$)	95.2	96.5	98.1	96.7	98.5	98.3	98.4	98.6	98.5	10.4	88.9 ± 27.6
VMT@40K ($\lambda_t = 0.02$)	60.6	60.5	58.8	47.3	59.9	53.3	55.4	52.8	47.0	14.6	51.0 ± 13.8
VMT@160K ($\lambda_t = 0.02$)	73.4	73.7	68.5	54.3	67.0	69.8	69.4	67.1	65.5	15.6	62.4 ± 17.3
VMT + DIRT-T@160K ($\lambda_t = 0.02$)	96.0	95.5	95.4	92.0	87.3	80.1	79.6	74.4	73.7	15.6	79.0 ± 23.9
VMT@40K ($\lambda_t = 0.01$)	57.7	57.6	57.4	50.1	54.1	50.0	52.7	40.1	53.9	45.5	51.9 ± 5.7
VMT@160K ($\lambda_t = 0.01$)	64.6	64.6	58.3	61.4	57.3	63.7	64.5	49.4	56.9	52.0	59.3 ± 5.5
VMT + DIRT-T@160K ($\lambda_t = 0.01$)	95.9	95.9	95.3	95.3	95.1	83.6	82.8	80.4	79.9	76.6	88.1 ± 8.0

Table 6: Comparison between $\lambda_t = 0.02$ and $\lambda_t = 0.01$ for MNIST \rightarrow SVHN without Instance-Normalized Input. VMT@40K:Source denotes the test set accuracy of VMT on the source domain at iteration 40000.

The Effect of λ_t for MNIST \rightarrow SVHN with Instance Normalization

Compared with VADA, we increase the value of λ_t for several tasks, as shown in Table 5. Because we find that increasing the value of λ_t can improve the performance significantly. But for VADA, it will collapse to a degenerate solution quickly if we set the same value of λ_t . Table 7 shows the results of $\lambda_t = 0.06$ and $\lambda_t = 0.01$ for MNIST \rightarrow SVHN with instance normalization, and we can observe that $\lambda_t = 0.06$ outperforms $\lambda_t = 0.01$ significantly.

MNIST \rightarrow SVHN with Instance-Normalized Input:											Average
VMT@40K($\lambda_t = 0.06$)	86.1	85.6	86.1	85.8	85.2	85.6	84.3	84.0	84.5	84.3	85.2 ± 0.8
VMT + DIRT-T@160K($\lambda_t = 0.06$)	96.0	95.9	95.6	95.5	95.4	95.3	95.3	95.1	94.2	92.8	95.1 ± 1.0
VMT@40K($\lambda_t = 0.01$)	72.8	75.3	74.8	74.4	73.7	72.3	72.3	73.8	73.9	71.7	73.5 ± 1.2
VMT + DIRT-T@160K($\lambda_t = 0.01$)	88.8	87.3	86.4	85.4	85.4	84.4	83.8	83.4	82.0	79.9	84.7 ± 2.6

Table 7: Comparison between $\lambda_t = 0.06$ and $\lambda_t = 0.01$ for MNIST \rightarrow SVHN with Instance-Normalized Input.

Comparing with Mixup on Intermediate Layers

In this experiment, we investigate the performance of mixup on intermediate layers. Table 8 shows the performance of mixup on the input of the last fully-connected layer. We also evaluated other intermediate layers, and mixup on logits performs the best.

MNIST \rightarrow SVHN with Instance-Normalized Input:											Average
VMT _{logits}	86.1	85.6	86.1	85.8	85.2	85.6	84.3	84.0	84.5	84.3	85.2 ± 0.8
VMT _{logits} + DIRT-T	96.0	95.9	95.6	95.5	95.4	95.3	95.3	95.1	94.2	92.8	95.1 ± 1.0
VMT _{inter}	85.5	83.9	84.0	84.1	77.9	74.2	70.8	47.4	32.4	16.3	65.7 ± 24.8
VMT _{inter} + DIRT-T	95.9	94.9	94.2	94.1	87.1	82.7	75.1	51.9	32.6	17.6	72.6 ± 28.6

Table 8: Comparison between mixup on logits and mixup on an intermediate layer.

Dynamic Accuracy Results of VAT and VMT

Compared with VAT, one advantage of VMT is the low computational cost. Figure 4 shows the dynamic results of the accuracy over time. We can observe that the model trained with VMT increases the accuracy much faster than the one trained with VAT.

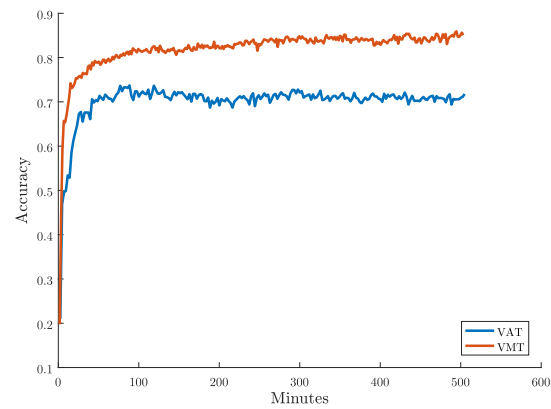


Figure 4: Dynamic test set accuracy on the adaptation task of MNIST \rightarrow SVHN with instance normalization. The blue line is for VAT and the red line is for VMT.